ELSEVIER

Orthogonal infrared dipole antenna

Peter Krenz [a], Javier Alda [b,*], Glenn Boreman [a]

[a] *CREOL/College of Optics and Photonics, University of Central Florida, 4000 Central Florida Blvd, Orlando, FL 32816-2700, USA*
[b] *Applied Optics Complutense Group, University Complutense of Madrid, School of Optics, Av. Arcos de Jalon s/n, 28037 Madrid, Spain*

Abstract

A dual-dipole structure is demonstrated at 10.6 μm, which facilitates electronic cancellation of the non-antenna-coupled thermal response of an infrared antenna-coupled bolometer. Structures of this type may also find utility in high-spatial-resolution measurement of Stokes parameters of a beam of radiation.
© 2007 Elsevier B.V. All rights reserved.

1. Introduction

The polarization response of an infrared antenna-coupled thermal sensor is strongly affected by the thermal and electrical characteristics of the surrounding structures, such as the substrate, lead lines, and bondpads [1–5]. For linearly polarized antennas such as dipoles, bowties, and logperiodics, the co-polarized response is identified with the antenna-coupled signal. The cross-polarized response originates with the electromagnetic coupling of signal extraction structures such as bondpads and leadlines, as well as with the heating of the structural substrate by laser irradiation or by Joule heating of the bolometer by the bias circuitry. However, these additional effects also contribute to the measured co-polarized signal, and a means to accurately remove this portion is desirable. This is especially true in the quantitative assessment of sensor-response mechanisms, when there are a number of response modes operating simultaneously [6].

In this contribution we demonstrate the operation of a pair of infrared dipole antennas, which are aligned orthogonal to each other and whose electrical outputs are wired so as to form a Wheatstone bridge. The combination of

the geometrical arrangement of the antennas and their internal and external electrical connections allows the co-polarized response to be isolated as the measured signal. Additionally, it is noted that for the case considered, this recorded signal is directly proportional to the S_1 Stokes parameter [7].

We also discuss briefly some possible extensions of the concept for measurement of additional Stokes parameters.

2. Experimental apparatus

As seen in Fig. 1, the experiment uses an orthogonal arrangement of two antenna-coupled bolometers. Infrared dipole A is oriented horizontally, and dipole B is vertical. They share a common connection at the point labeled V_G in the diagram. The length of the dipole was chosen to maximize response at a wavelength of 10.6 μm [8]. The structure including substrate and bondpads was modeled using Ansoft HFSS. As seen in Fig. 2, a full length of 1.55 μm was chosen as the point where the imaginary part of the dipole impedance goes through a zero.

The devices were fabricated on a high resistivity (3–6 kΩ cm) Silicon wafer using direct-write e-beam lithography. The dipole antenna and bondpads are 75-nm-thick e-beam evaporated gold with a 5 nm Titanium adhesion layer, while the bolometer is 80 nm of e-beam evaporated

* Corresponding author. Tel.: +34913946874; fax: +34913946885.
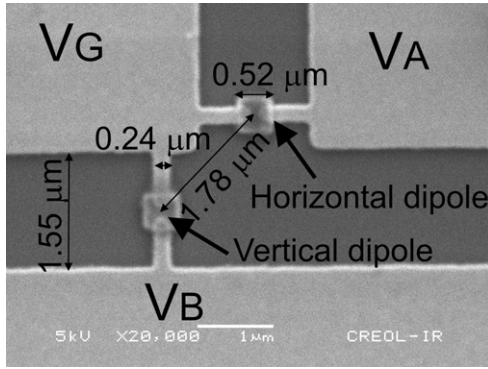*E-mail address:* j.alda@opt.ucm.es (J. Alda).

Fig. 1. Scanning electron micrograph of the on-chip arrangement of the pair of orthogonal dipole antennas.

Fig. 3. Schematics of the on-chip and off-chip wiring of the devices. The dipoles are arranged as part of a Wheatstone bridge. The output of the bridge is externally balanced by using a variable gain, α, in one of the amplifiers.
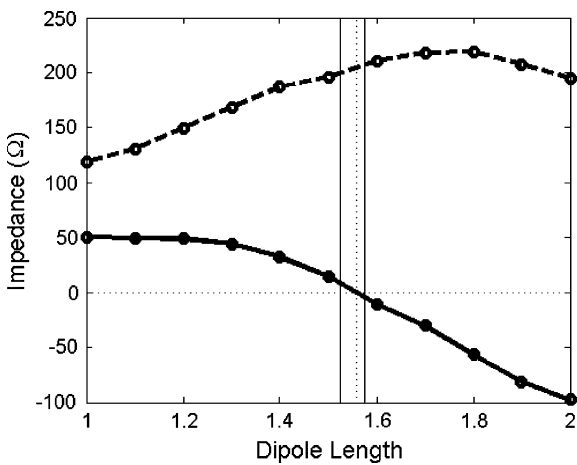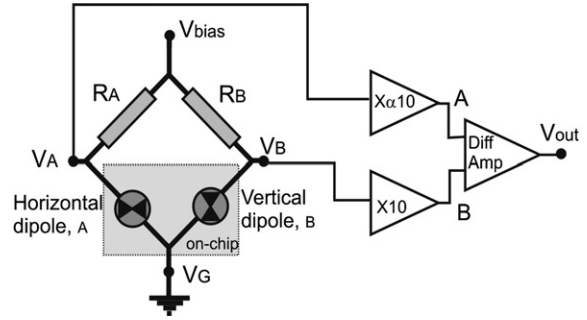

Fig. 2. Real (dashed line) and imaginary (solid line) impedance for the dipole and bondpads arrangement as a function of the length of the dipole. The circles correspond to the values obtained from numerical modeling. The vertical solid lines represent the range of the dipole lengths obtained in the fabrication. The dashed vertical line corresponds with the zero-crossing of the imaginary part of the impedance.

nickel. The distance between the centers of the two orthogonal dipoles was varied (1.33, 1.78, and 2.05 μm in devices 1, 2, and 3, respectively), to examine any influence on the overall behavior of the element. A smaller distance might be expected to exhibit a higher electromagnetic crosstalk, as the price paid for a more compact measurement aperture. The bolometer DC resistance in each device was different because of lithographic differences. These resistances were 40.3, 34.1, and 24.4 ohm, respectively for the studied devices.

Fig. 3 shows that the interconnection between the two antenna-coupled sensors, along with the external biasing electronics, configures a Wheatstone bridge. The response of each sensor consists of several contributions: a substrate-heating thermal response that is not polarization sensitive, residual electromagnetic crosstalk between the antennas themselves and between the antennas and the bondpads, and the dipole-antenna-coupled response, which is the term that we want to extract. The Wheatstone bridge arrangement is able to compensate the thermal response of the elements. Any electromagnetic crosstalk will be the same for both two antennas because of the geometrical symmetry of the layout.

Both bolometers (A and B) are biased using the same voltage, V_{bias} and resistors of equal value, $R_A = R_B$. The DC resistances of the individual bolometers are slightly different, which unbalances the Wheatstone bridge, even when it is not illuminated. The voltage signals V_A, V_B obtained from the bridge are fed to two independent amplifiers. The gain of one amplifier is variable (α), which allows the output of the bridge to be externally balanced, yielding a differential voltage, $V_{out} = 10 \times (\alpha V_A - V_B)$. A dual-channel lock-in amplifier operating in differential mode is used to measure V_{out}, at a chopping frequency of 2.5 kHz. This configuration allows cancellation of the cross-polarized response of the antenna. The remaining signal will be the dipole-antenna-coupled portion of the response, which should be proportional to the projection of the electric field along the dipole direction.

The light source used for the characterization of the devices is a CO_2 laser emitting at 10.6 μm. The Gaussian full width of the spot at the plane of the antennas is 150 μm ± 20 μm, illuminating the antenna pair quasi-uniformly. The polarization of the laser is linear with an azimuth angle θ, which can be rotated using a λ/2 wave plate. An incident beam polarized in the horizontal direction is defined as θ = 0°. The total power falling on the devices is adjustable. A reference detector is placed in a separate optical channel to allow calibration of laser-power fluctuations. The differential voltage signal obtained from the detectors, V_{out}, is normalized to the reference laser power, P, to produce the responsivity $\mathcal{R}_{out} = V_{out}/P$, having dimensions of [V/W]. To balance the Wheatstone bridge, the polarization of the incident light is set to 45°. Then the gain α of the variable amplifier is adjusted in order to cancel the differential signal.

3. Results and discussion

We measured the three pairs of orthogonal dipoles, for which the distance between the centers of the dipoles was

noted above. The responsivity $\mathscr{R}_{out}$, vs. θ is expected to follow the polarization angle, θ, as a harmonic function, and is plotted in Fig. 4 for the three devices. Device #3 has been illuminated at half the power (50 mW) of devices #1 and #2 (100 mW). The differences in resistance between the three result in the observed magnitude difference of $\mathscr{R}_{out}$. The distance between the centers of the dipoles does not seem to produce a noticeable effect on the measured response of the dipole pair, since the variations of the distance remain in the sub-wavelength range.

The variation of $\mathscr{R}_{out}$ with respect to the azimuth angle can be modeled as

$$\mathscr{R}_{out} = \mathscr{R}_0 \cos[2(\theta - \theta_0)] - \mathscr{R}_{offset}, \qquad (1)$$

where $\mathscr{R}_0$ accounts for the amplitude of $\mathscr{R}_{out}$, θ_0 represents a small shift due to angular misalignments and angular positioning errors in the polarization elements, and $\mathscr{R}_{offset}$ represents a constant residual level. This $\mathscr{R}_{offset}$ should be as small as possible and can be minimized by properly balancing the outputs of the Wheatstone bridge. The values of these parameters that best fit the experimental data are shown in Table 1. The value of the correlation coefficient
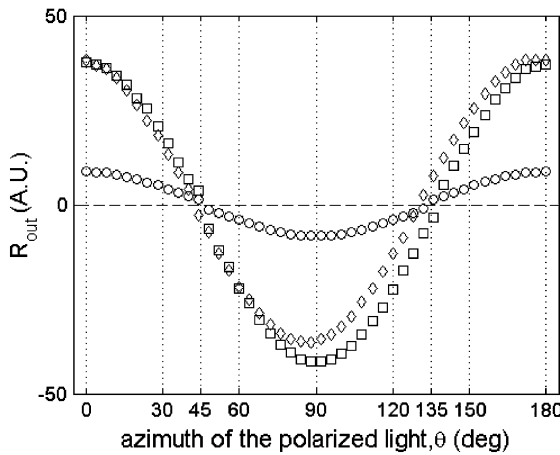
[9] shows how well the experimental data fits the model expressed in Eq. (1).

Using the signals obtained from the devices, it is possible to obtain an experimental value of the normalized S_1 Stokes parameter. Following the definition of the S_1 Stokes parameter in terms of the electric field amplitudes, $S_1 = |E_x|^2 - |E_y|^2$, we see that the output obtained from the lock-in amplifier working in differential mode, V_{out}, is directly proportional to S_1. Also, since $\mathscr{R}_{out}$ contains a normalization to the total power of the beam, and considering the definition of the Stokes parameter $S_0 = |E_x|^2 + |E_y|^2$, we find that $\mathscr{R}_{out}$ is proportional to the normalized $s_1 = S_1/S_0$ parameter. The value of the amplitude $\mathscr{R}_0$ in Eq. (1) can be seen as the proportionality constant between $\mathscr{R}_{out}$ and s_1 (assuming that $\mathscr{R}_{offset}$ can be cancelled by proper adjustment of the Wheatstone bridge). This value can be alternatively obtained directly from the measurements of the individual elements of the pair. Table 2 shows the maximum and minimum values of the measured normalized quantity obtained individually for the horizontally and vertically oriented dipoles. The minimum value is assumed to be caused by the thermal response of the device. These values are not equal for both elements in a given dipole pair due to slight variations in the impedance of the elements resulting from fabrication tolerances.
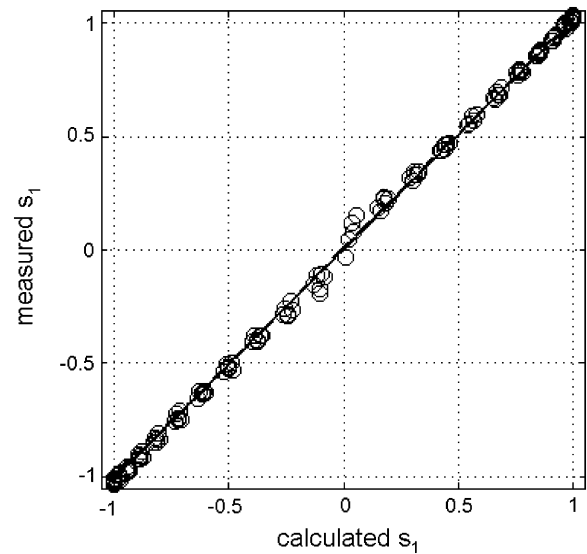

Fig. 4. Variation of $\mathscr{R}_{out}$ as a function of the azimuth of the linearly polarized light illuminating the device. The power level for devices #1 (diamonds) and #2 (squares) is double than for device #3 (circles).

Fig. 5. Plot of the normalized Stokes parameter S_1 obtained from the measurements vs. the theoretically calculated S_1 parameter. A total of 138 measurements are shown as circles. The linear fitting of these values is shown as a dashed line.

Table 1
Parameters of the fitting of the responsivity vs angle (Eq. (1))

Device	$\mathscr{R}_0$	$\mathscr{R}_{offset}$	θ_0 (deg)	Correlation coefficient
#1	37.4	−1.1	−1.84	0.9920
#2	39.6	2.1	0.31	0.9994
#3	8.6	0.0	0.00	0.9993

Table 2
Experimental values of the responsivities used in Eqs. (2) and (3)

Device	$\mathscr{R}_{hor,max}$	$\mathscr{R}_{hor,min}$	$\mathscr{R}_{ver,max}$	$\mathscr{R}_{ver,min}$	$\mathscr{R}_{0,exp}$	$\mathscr{R}_{offset,exp}$
#1	79.4 ± 0.4	47.6 ± 0.3	84.9 ± 0.2	42.9 ± 0.2	36.9 ± 0.5	−0.4 ± 0.5
#2	83.3 ± 0.2	31.6 ± 0.3	68.3 ± 0.1	43.4 ± 0.1	38.3 ± 0.4	1.6 ± 0.4
#3	33.5 ± 0.3	22.1 ± 0.1	30.4 ± 0.2	25.3 ± 0.2	8.3 ± 0.4	0.1 ± 0.4

We have evaluated the amplitude $\mathscr{R}_{0,exp}$ from the experimental measurements given in Table 2 as the average of the pure polarized responses obtained for linearly polarized light oriented at 0° (horizontal) and 90° (vertical) as,

$$\mathscr{R}_{0,exp} = \frac{1}{2}[(\mathscr{R}_{hor,max} - \mathscr{R}_{ver,min}) + (\mathscr{R}_{ver,max} - \mathscr{R}_{hor,min})]. \quad (2)$$

This amplitude is the proportionality factor that it is necessary to transform the values of $\mathscr{R}_{out}$ into s_1. The value of $\mathscr{R}_{offset}$ is also obtained from this table as

$$\mathscr{R}_{offset,exp} = \frac{1}{2}[(\mathscr{R}_{hor,max} - \mathscr{R}_{ver,min}) - (\mathscr{R}_{ver,max} - \mathscr{R}_{hor,min})]. \quad (3)$$

Both $\mathscr{R}_{0,exp}$ and $\mathscr{R}_{offset}$, exp are expressed in the last column of Table 2 along with the error calculated from the experimental data.

Fig. 5 shows the value of s_1 evaluated from the measurements *vs.* the expected value as analytically calculated from the polarization state illuminating the devices. The linear fitting shows a correlation factor of 0.9999. The poorest experimental evaluation of s_1 appears around $s_1 = 0$, which correspond to values of the signal close to zero. This is due to the noise level of the devices and external electronics, and the uncertainties associated with the balancing of the Wheatstone bridge.

4. Conclusions

The use of two orthogonal optical dipole antennas which are electrically connected to form a Wheatstone bridge has been demonstrated experimentally. The dependence of the functional form of the response of the devices with the distance between the bolometer has been shown to be negligible for the cases studied. The advantage of the orthogonal dipole arrangement is the cancellation of the cross-polarization response of an individual dipole antenna, which is mainly caused by the excitation of a polarization independent thermal response. The output of the device has been processed to obtain the s_1 parameter for a linearly polarized incident beam in the infrared.

From previous studies [3] the spatial extent of the antenna-coupled response is very closely associated with the resonant structures. Because of the inherent cancellation of the cross-polarized response, it is expected that the spatial response of this device should be even smaller than the one of a single dipole antenna, allowing high spatial resolution measurements.

Possible extensions of this work include the setting of another couple of orthogonal dipoles oriented at 45 with

respect to the horizontal direction to determine the third Stoke parameter s_2 [7,10]. The integration of a $\lambda/4$ waveplate [11] properly oriented with respect to the dipoles may be used to determine the fourth Stokes parameter, s_3. Alternatively, if spiral antennas are similarly arranged and connected as the dipoles shown in this paper, s_3 could be determined experimentally. All these measurements would also take advantage of the high spatial resolution associated with the use of infrared antennas.

References

[1] J. Alda, C. Fumeaux, M. Gritz, D. Spencer, G. Boreman, Responsivity of infrared antenna-coupled microbolometers for air-side and substrate-side illumination, Infrared Phys. Technol. 41 (2000) 1–9.
[2] I. Codreanu, G. Boreman, Influence of dielectric substrate on the responsivity of microstrip dipole-antenna-coupled infrared microbolometers, Appl. Opt. 41 (2002) 1835–1840.
[3] J. Alda, C. Fumeaux, I. Codreanu, J. Schaefer, G. Boreman, Deconvolution method for two-dimensional spatial-response mapping of lithographic infrared antennas, Appl. Opt. 38 (1999) 3993–4000.
[4] C. Fumeaux, W. Herrmann, F. Kneubühl, Nanometer thin film Ni–NiO–Ni diodes for detection and mixing of 30 THz radiation, Infrared Phys. Technol. 38 (1998) 123–183.
[5] C. Fumeaux, J. Alda, G. Boreman, Lithographic antennas at visible frequencies, Opt. Lett. 24 (1999) 1629–1631.
[6] H. Kazemi, K. Shinohara, G. Nagy, W. Ha, B. Lail, E. Grossman, G. Zummo, W. Folks, J. Alda, G. Boreman, First THz and IR characterization of nanometer-scaled antenna-coupled InGaAs/InP Schottky-diode detectors for room temperature infrared imaging, Proc. SPIE 6542 (2007).
[7] R. Azzam, N.M. Bashara, Ellipsometry and Polarized Light, Elsevier, 1988.
[8] C. Fumeaux, M. Gritz, I. Codreanu, W. Schaich, F.J. Gonzalez, G. Boreman, Measurement of resonant lengths of infrared dipole antennas, Infrared Phys. Technol. 41 (2000) 271–281.
[9] M.R. Spiegel, Correlation Theory. Ch. 14 in Theory and Problems of Probability and Statistics, second ed., McGraw-Hill, New York, 1992.
[10] Y. Liu, G.A. Jones, Y. Peng, T.H. Shen, Generalizad theory and application of Stokes parameter measurements made with a single photoelastic modulator, J. Appl. Phys. 100 (2006) 063537.
[11] J. Tharp, J. Lopez-Alonso, J. Ginn, B. Lail, C. Middleton, B. Munk, G. Boreman, Demonstration of a Single Layer Meanderline Phase Retarder at IR, Opt. Lett. 31 (2006) 2687–2689.